Evolutionary patterns of chromosomal instability and mismatch repair deficiency in proximal and distal colorectal cancer

Monika M. Golas, Bastian Gunawan, Meliha Cakir, Silke Cameron, Christina Enders, Torsten Liersch, Laszlo Füzesi, Bjoern Sander

Angaben zur Veröffentlichung / Publication details:

Golas, Monika M., Bastian Gunawan, Meliha Cakir, Silke Cameron, Christina Enders, Torsten Liersch, Laszlo Füzesi, and Bjoern Sander. 2022. "Evolutionary patterns of chromosomal instability and mismatch repair deficiency in proximal and distal colorectal cancer." *Colorectal Disease* 24 (2): 157–76. https://doi.org/10.1111/codi.15946.

Received: 31 January 2021 | Revised: 4 July 2021 | Accepted: 28 September 2021

DOI: 10.1111/codi.15946

ORIGINAL ARTICLE

Evolutionary patterns of chromosomal instability and mismatch repair deficiency in proximal and distal colorectal cancer

Mariola Monika Golas[1] | Bastian Gunawan[2] | Meliha Cakir[2] | Silke Cameron[3] | Christina Enders[2] | Torsten Liersch[4] | Laszlo Füzesi[2,5] | Bjoern Sander[2,6]

[1]Department of Hematology and Medical Oncology, Comprehensive Cancer Center Augsburg, University Medical Center Augsburg, Augsburg, Germany

[2]Institute of Pathology, University Medical Center Göttingen, Göttingen, Germany

[3]Department of Gastroenterology and Gastrointestinal Oncology, University Medical Center Göttingen, Göttingen, Germany

[4]Department of General, Visceral and Pediatric Surgery, University Medical Center Göttingen, Göttingen, Germany

[5]Institute of Pathology and Molecular Diagnostics, University Medical Center Augsburg, Augsburg, Germany

[6]Institute of Pathology, Hannover Medical School, Hannover, Germany

Correspondence
M. Monika Golas, Department of Hematology and Medical Oncology, Comprehensive Cancer Center Augsburg, University Medical Center Augsburg, Augsburg, Germany.
Email: monika.golas@med.uni-augsburg.de

Funding information
University of Augsburg; University Medical Center Göttingen

Abstract

Aim: Colorectal carcinomas (CRCs) progress through heterogeneous pathways. The aim of this study was to analyse whether or not the cytogenetic evolution of CRC is linked to tumour site, level of chromosomal imbalance and metastasis.

Method: A set of therapy-naïve pT3 CRCs comprising 26 proximal and 49 distal pT3 CRCs was studied by combining immunohistochemistry of mismatch repair (MMR) proteins, microsatellite analyses and molecular karyotyping as well as clinical parameters.

Results: A MMR deficient/microsatellite-unstable (dMMR/MSI-H) status was associated with location of the primary tumour proximal to the splenic flexure, and dMMR/MSI-H tumours presented with significantly lower levels of chromosomal imbalances compared with MMR proficient/microsatellite-stable (pMMR/MSS) tumours. Oncogenetic tree modelling suggested two evolutionary clusters characterized by dMMR/MSI-H and chromosomal instability (CIN), respectively, for both proximal and distal CRCs. In CIN cases, +13q, −18q and +20q were predicted as preferentially early events, and −1p, −4 -and −5q as late events. Separate oncogenetic tree models of proximal and distal cases indicated similar early events independent of tumour site. However, in cases with high CIN defined by more than 10 copy number aberrations, loss of 17p occurred earlier in cytogenetic evolution than in cases showing low to moderate CIN. Differences in the oncogenetic trees were observed for CRCs with lymph node and distant metastasis. Loss of 8p was modelled as an early event in node-positive CRC, while +7p and +8q comprised early events in CRC with distant metastasis.

Conclusion: CRCs characterized by CIN follow multiple, interconnected genetic pathways in line with the basic 'Vogelgram' concept proposed for the progression of CRC that places the accumulation of genetic changes at centre of tumour evolution. However, the timing of specific genetic events may favour metastatic potential.

KEYWORDS
aneuploidy, chromosomal instability, clonal evolution, colorectal cancer, copy number aberrations, microsatellite instability, oncogenetic tree model, Vogelgram

INTRODUCTION

Colorectal cancer (CRC) is one of the most common types of cancer in both women and men [1,2]. This malignancy represents a heterogeneous group of tumours with regard to clinical, morphological and pathogenetic characteristics [3–5]. CRC has been suggested to comprise a proximal, right-sided subtype that arises in the midgut-derived part of the large bowel and a distal, left-sided subtype arising in the hindgut-derived bowel [3], although transitions of the phenotype may be gradual [6]. Compared with left-sided CRCs, right-sided CRCs show a moderate female predominance and the mean age at diagnosis is higher [7]. Mucinous or undifferentiated phenotypes are preferentially observed in right-sided CRCs, and the disease stage appears to be more advanced [7]. A site preference has also been observed for CRCs related to tumour predisposition syndromes. In patients with Lynch syndrome, CRCs typically occur in the right-sided colon [8]. In the distal colon and rectum, familial adenomatous polyposis coli syndrome (FAP)-associated CRC appears to be more common, although FAP patients may also develop CRC in the right-sided colon [8].

It is established that CRC develops through several pathways resulting in different cytogenetic and molecular characteristics of the tumour [9]. The largest subset of CRCs evolves through chromosomal instability (CIN), which results in common chromosomal aberrations including losses at 8p, 17p and 18q as well as gains at 7p, 7q, 8q, 13q and 20q, and more variably losses at 1p, 4p, 4q, 5q, 14q, 15q and 18p as well as gains at 1q and 20p [10–17]. In contrast, CRCs with a high degree of microsatellite instability (MSI-H) [18–20] often present with a stable, near-diploid karyotype, although some MSI-H tumours show chromosomal imbalances as well [21–25]. MSI-H is characterized by disruption of the DNA mismatch repair (MMR) system that maintains DNA sequence fidelity [26]. In Lynch syndrome, germline pathogenic variants in any of the MMR genes *MLH1*, *MSH2*, *MSH6* and *PMS2*, or in *EPCAM* (deletions in the latter non-MMR gene result in silencing of the adjacent MMR gene *MSH2* [27]), predispose to the development of CRC with an MSI-H phenotype [28–31]. In sporadic CRCs, MMR deficiency is caused by expression loss of MMR genes, which commonly originates from epigenetic silencing of the *MLH1* gene by promoter methylation [32–34]. *MLH1* promoter methylation correlates with a high CpG island methylator phenotype (CIMP-H) [35]; however, methylation of the *MLH1* promoter also occurs in CIMP-negative or CIMP-low tumours [36].

In a collaborative effort, the CRC Subtyping Consortium suggested a stratification of CRCs into the following four consensus molecular subtypes (CMS) [9]. (1) Tumours belonging to CMS1 – the MSI immune subtype – share MSI-H, CIMP-H and a hypermutation phenotype; these tumours commonly harbour *BRAF* mutations and are characterized by activation of immune cells [9]. (2) CIN is predominant in CMS2 tumours (canonical subtype), which reveal activation of *MYC* and the WNT pathway [9]. (3) In CMS3, metabolic deregulation dominates the phenotype; both CIN and CIMP status are low, and tumours typically harbour *KRAS* mutations. (4) The mesenchymal subtype, CMS4, shares CIN with CMS2, but demonstrates activation of the transforming growth factor beta pathway [9]. Mixed subtypes may be observed in a minority of CRCs [9].

What does this paper add to the literature?

This paper addresses the tumour evolution of colorectal cancer (CRC) and demonstrates that in addition to the mismatch repair-deficient/microsatellite-unstable pathway, CRCs characterized by chromosomal instability follow different, interconnected genetic pathways. These results provide evidence for the 'Vogelgram' concept, which indicates that accumulation of genetic alterations dictates tumour evolution, but also suggest a role for the timing of the genetic events.

Several models have been put forward to describe the temporal order of genetic alterations acquired during the development of CRC. In 1990, Fearon and Vogelstein linked recurrent genetic alterations to the adenoma-to-carcinoma sequence [37]. In their progression model, commonly referred to as the 'Vogelgram', colorectal tumourigenesis is typically initiated by the loss of *APC* favouring hyperproliferation of the intestinal epithelium, followed by somatic mutations in *KRAS*, loss of 18q as well as loss of *TP53*, ultimately resulting in invasive cancer [37]. The Vogelgram model, however, should be interpreted as preferred, but not the exclusive order of genetic events (i.e. the genetic alterations may occur in any order) [37]. Later, the MSI-H pathway was integrated into the progression model of CRC as a distinct pathway separated from the Vogelgram pathway [38]. The basic concept of the evolutionary model was corroborated in a recent study of the International Cancer Genome Consortium/The Cancer Genome Atlas (ICGC/TCGA) Pan-Cancer Analysis of Whole Genomes (PCAWG) Consortium, which devised driver mutations in *APC*, *KRAS*, *PIK3CA*, *TP53* and *FBXW7* as well as the chromosomal imbalances +8q, −17p and −18q as preferentially early events [39]. The aim of the present study was to address whether or not the cytogenetic evolution of CRC is specific for certain tumour characteristics. To this end, oncogenetic trees were reconstructed for CRCs using maximum likelihood estimation [40] and maximum-weight branching approaches [41,42] to model the evolution of common chromosomal imbalances and the MMR/microsatellite (MS) status in proximal and distal CRCs.

METHOD

Study cohort

This study was approved by the local ethics committee. Ethics approval was obtained for all cases included in the study. To minimize differences related to tumour stage, only locally advanced (pT3) CRCs were included in the current series. The cohort comprised 75 primary CRCs, including 26 proximal CRCs (located in the caecum,

ascending colon, hepatic flexure or colon transversum) and 49 distal CRCs (located in the rectum, i.e. aboral tumour margin up to 16 cm from the anal verge). Pathological staging was performed according to the recommendations of the Union for International Cancer Contro (UICC) published in 2016 [43]. Primary resection of all CRCs was performed. Patients diagnosed with clinical UICC Stage IV CRC underwent surgery of the primary tumour as well as of resectable liver metastasis with potentially curative intent as a single case decision after discussion in a multiprofessional interdisciplinary tumour board. Patients with locally advanced rectal cancers (clinically staged as UICC Stages II and III) were treated within or according to the control arm of the CAO/ARO/AIO-94 phase III trial of the German Rectal Cancer Study Group with primary surgery, typically followed by postsurgery fluorouracil (5-FU)-based chemoradiotherapy or 5-FU monotherapy [44,45]. Thus, only naïve tumour material was analysed in this study, i.e. the tumour material was obtained prior to any postoperative irradiation and/or chemotherapy. Vital status was available for all patients; complete information on patient follow-up (mean 39 months, median 40 months, maximum 103 months) was available for 70 patients. Overall survival (OS) was the time between surgical treatment and the date of death, irrespective of cause.

Immunohistochemical MMR analysis

Immunohistochemical studies on formalin-fixed, paraffin-embedded tumour tissue were performed for MLH1 (clone G168-15; BD Biosciences, Franklin Lakes, NJ, USA; dilution 1:50; microwave pretreatment), MSH2 (clone FE11, Zytomed Systems GmbH, Berlin, Germany; dilution 1:50; microwave pretreatment), MSH6 (clone 44, BD Biosciences; dilution 1:50; microwave pretreatment) and PMS2 (clone A16-4, BD Biosciences; dilution 1:50; microwave pretreatment) using the DAKO ChemMate™ Detection Kit (Dako, Glostrup, Denmark) for visualization. Noncancerous intestinal crypt cells, lymph follicles and stromal cells served as internal controls for the staining reactions. Negative protein expression of the respective MMR protein was defined as complete loss of nuclear staining within the tumour. Immunohistochemical slides were evaluated without knowledge of the MSI results. Tumours with aberrant staining loss of a pair of MMR proteins or individual loss of PMS2 or MSH6 were classified as MMR deficient (dMMR), while tumours with no loss of staining were classified as MMR proficient (pMMR).

MSI analysis

For selected cases, analysis of microsatellites was performed on DNA extracted from formalin-fixed and paraffin-embedded tissue blocks. We used the Promega MSI Multiplex System Version 1.2 (Promega, Madison, WI, USA) according to the manufacturer's instructions, which offers five nearly monomorphic mononucleotide repeat markers (BAT-25, BAT-26, NR-21, NR-24 and MONO-27) for MSI determination and two polymorphic pentanucleotide markers (Penta C and Penta D) for sample identification. Products were separated by capillary electrophoresis using an ABI 3100 Genetic Analyser (Applied Biosystems, Foster City, CA, USA). Tumours with MSI at two or more mononucleotide loci were stratified as MSI-H, while tumours with MSI at a single mononucleotide locus were MSI-low (MSI-L) and tumours with no MSI at any of the loci tested were MS-stable (MSS) [46].

Analysis of chromosomal imbalances

Tumour DNA was isolated from formalin-fixed and dewaxed tumour tissue sections and analysed by comparative genomic hybridization (CGH) as detailed previously [47]. The Quips Karyotyping/CGH software suite (Vysis, Downers Grove, IL, USA) was used to obtain green-to-red fluorescence ratios for each metaphase chromosome. Gains, high-level amplifications and losses were defined as chromosomal regions where the average green-to-red fluorescence ratio was >1.2, >2 and <0.8, respectively. In exceptional cases, where the aforementioned thresholds were not met, deviations from normal were classified as gains or losses when the 95% confidence interval varied beyond the ratio of 1.0. The following chromosomal regions that are known for false results were not included in the analysis: 1p32pter, 13p, 14p, 15p, 21p, 22p, telomeres and constitutive heterochromatic regions at 1q, 9q, 16q and Yq [48]. Aneuploidy scores were used to quantify chromosomal arm aneuploidy and calculated as the total number of chromosomal arms with an apparent whole arm gain or loss [49]. Short arms of acrocentric chromosomes (i.e. chromosomes 13, 14, 15, 21 and 22) were not included in the aneuploidy score.

Statistical analysis

Statistical analyses were performed using the software platform R [50]. Fisher's exact test for contingency tables was used to analyse clinico-pathological parameters. For the statistical test of net changes and aneuploidy score versus localization, the two-sided Wilcoxon rank sum test with continuity correction was selected as the Shapiro–Wilk normality test indicated nonnormally distributed data. The Mantel–Haenszel log-rank test for censored data was selected for the correlation of clinico-pathological characteristics and individual imbalances identified in the tumours. Survival was estimated using Kaplan–Meier curves. The Benjamini–Hochberg method was used to correct for multiple testing. A p-value <0.05 was considered statistically significant.

Oncogenetic tree models

An oncogenetic tree model using maximum likelihood estimation [40] was reconstructed using the entire study cohort, i.e. independent of the tumour location. To this end, the R package 'oncomodel'

(https://cran.r-project.org/web/packages/oncomodel/index.html) was selected. The MS status as well as the most common chromosomal imbalances observed in the cohort were included in the modelling. Additionally, maximum-weight branching oncogenetic tree models [41,42] were separately computed for proximal and distal CRCs using the R package 'OncoTree' (https://cran.r-project.org/web/packages/Oncotree/index.html), as were oncogenetic trees for CRCs stratified according to the number of chromosomal imbalances (with categories ≤10 and >10 being aberrations), the node status (with categories pN0, pN1a/b, pN2a/b) and presence or absence of distant metastasis (with categories no metastasis, synchronous metastasis, metachronous metastasis).

RESULTS

Clinico-pathological characteristics of the patient cohort

The study included 75 patients with primary CRC (Table 1). The age of the patients at the time of diagnosis ranged from 29 to 87 years (mean 64.4 years) in the proximal CRC group and from 44 to 89 years (mean 68.6 years) in the distal CRC group. There were 31 women and 44 men in our cohort. Twenty six patients (35%) had a CRC proximal to the splenic flexure and 49 (65%) a distal CRC. Among the 26 patients with proximal pT3 CRCs, 10 (38%) were in clinical Stage IIA (pN0), 7 (27%) in clinical Stage IIIB (pN1 or pN2a), 1 (4%) in clinical Stage IIIC (pN2b) and 8 (31%) in clinical Stage IVA (M1a). Among the 49 patients with distal pT3 CRC, 23 (47%) were in clinical Stage IIA, 10 (20%) in clinical Stage IIIB, 12 (24%) in clinical Stage IIIC, 3 (6%) in clinical Stage IVA and 1 (2%) in clinical Stage IVB (M1b).

There were significant differences in the rate of synchronous versus metachronous metastatic disease between the proximal and distal CRCs ($p = 0.02$, Fisher's exact test). In particular, proximal CRCs were more likely to show synchronous metastasis [8/26 (31%) vs. 4/49 (8%) of the distal CRCs], while metachronous metastasis was predominantly observed in distal CRCs stratified as cM0 at initial cancer staging [1/17 (6%) of the proximal CRCs vs. 9/40 (23%) of the distal CRCs]. A positive node status ($p = 2.9 \times 10^{-6}$) and the disease stage ($p = 1.7 \times 10^{-4}$, log rank/Mantel–Haenzel test) were significant predictors of OS (Figure 1). However, we did not observe a significant difference in the OS between the proximal and the distal CRCs ($p > 0.05$). Likewise, no significant differences in the OS were noted between the proximal and the distal tumour site among patients with tumours of the same clinical stage ($p > 0.05$ for clinical Stage II, III and IV).

MMR protein expression and microsatellite analysis

Immunohistochemically, 65 of the tumours (87%) showed nuclear expression of the MMR proteins MLH1, MSH2, MSH6 and PMS2 (Table 1). In the remaining 10 tumours, there was complete absence of nuclear staining for at least one MMR protein. Specifically, loss of expression was observed for PMS2 in 8 (11%) cases, for MLH1 in 6 (8%) cases, for MSH6 in 2 (3%) cases and for MSH2 in 1 (1%) case (Table 1). Isolated loss of expression of PMS2 and MSH6 was found in two tumours and one tumour, respectively. There was concurrent negative expression of MLH1/PMS2 in six cases, representing 100% of MLH1-negative cases and 75% of PMS2-negative cases. Concurrent negative expression of MSH2/MSH6 was observed in one tumour.

For ten selected cases, the MS status was determined by complementary MSI analysis. In all but one case, the MS status indicated by the immunohistochemical analysis of the MMR proteins was confirmed by the MSI analysis. However, one tumour showing loss of PMS2 expression and an above average level of DNA copy number aberrations (case 16 with 14 chromosomal imbalances) was reclassified as MS-stable based on the result of the MSI analysis. Thus, with complementary MSI analysis, 66 tumours were classified as pMMR/MSS and 9 tumours as dMMR/MSI-H, representing 27% of the proximal CRCs and only 4% of the distal CRCs (7/26 vs. 2/49; $p = 0.02$; Fisher's exact test). Overall, there were no significant differences in the OS when the dMMR/MSI-H and pMMR/MSS tumours were compared ($p > 0.05$; log rank/Mantel–Haenzel test).

Chromosomal imbalances

DNA copy number aberrations were detected in 66 of the 75 CRC cases (88%) (Figure 2; details are provided in Table 1). The two most common autosomal imbalances were +20q (61%) and −18q (60%), followed by, in decreasing frequency, +13q (45%), +8q (35%), −8p (33%), −4q (31%), −18p (27%), +20p (27%), −4p (23%), −14q (23%), −1p, (20%), +7p (20%), −5q (19%), −17p (19%), +12p (16%) and −15q (16%) (Figure 2).

Proximal pT3 CRCs revealed a significantly lower number of chromosomal imbalances than distal pT3 CRCs (mean 5.3 vs. 8.8; $p = 0.02$; Wilcoxon test; Table 2), including fewer gains and amplifications (mean 2.8 vs. 4.1; $p = 0.047$; Wilcoxon test) and fewer losses (mean 2.4 vs. 4.6; $p = 0.03$; Wilcoxon test). There was a trend toward higher rates of karyotypes devoid of apparent chromosomal imbalances in proximal CRCs compared with distal CRCs (6/26 vs. 3/49; $p = 0.08$; Fisher's exact test). The significantly lower number of chromosomal imbalances observed in proximal CRCs appeared to be correlated with the higher frequency of proximal CRCs showing the dMMR/MSI-H phenotype. When the proximal and distal CRCs were compared according to the MMR/MS status, no significant differences in the number of chromosomal imbalances were seen for the proximal and distal CRCs ($p > 0.05$ for the pMMR/MSS and dMMR/MSI-H cases; Wilcoxon test; Table 2).

The majority of the CRCs (i.e. 62 tumours, 83%) analysed in this study showed chromosome arm aneuploidy defined as at least one imbalance that apparently encompassed the whole chromosome arm. Aneuploidy scores were separately determined for both the proximal and distal CRCs (Table 2). As for the total number of chromosomal

TABLE 1 Clinico-pathological and genetic findings in 75 primary colorectal carcinomas

No.	Age (years)/ sex	Site	pN	Clinical stage	Follow-up, OS (months)	MS analysis	MMR immunohistochemistry				MMR/MS status	Aneuploidy score	Gains	Losses
							MLH1	MSH2	MSH6	PMS2				
1	72/F	Colon asc	0	IIA	NED, 80	MSS	+	+	+	+	pMMR/MSS	0	0	0
2	29/M	Colon asc	0	IIA	NED, 46	MSI-H	+	−	−	+	dMMR/MSI	0	0	0
3	61/F	Colon asc	0	IIA	NED, 66	MSI-H	−	+	+	−	dMMR/MSI	0	0	0
4	84/M	Caecum	0	IIA	DOTD (DP), 15 (NA)	MSI-H	−	+	+	−	dMMR/MSI	0	0	0
5	76/M	Colon transv	0	IIA	DOO, 6	NA	+	+	+	+	pMMR/MSS	0	0	−10q
6	53/M	Caecum	0	IIA	NED, 78	NA	+	+	+	+	pMMR/MSS	0	+12p, +12q	0
7	67/F	Colon asc	0	IIA	NED, 75	NA	+	+	+	+	pMMR/MSS	3	+13q, +20p, +20q	−17p
8	34/F	Colon asc	0	IIA	NED, 50	NA	+	+	+	+	pMMR/MSS	8	+6p, +7p, +7q, +9p, +13q	−4p, −4q, −8p, −18p, −18q
9	87/M	Colon asc	0	IIA	DOO, 38	NA	+	+	+	+	pMMR/MSS	7	+2p, +2q, +6p, +8q, +17q, +20q	−3p, −5q, −8p, −17p, −18q
10	68/M	Colon transv	0	IIA	NED, 35	NA	+	+	+	+	pMMR/MSS	7	+7p, +7q, +9q, +13q, +18p, +20p, +20q, +Xp, +Xq	−9p, −18q
11	52/M	Colon transv	1a	IIIB	NED, 69	MSI-H	−	+	+	−	dMMR/MSI	0	0	0
12	87/M	Colon asc	1a	IIIB	DOO, 4	NA	+	+	+	+	pMMR/MSS	1	+20q	0
13	80/M	Colon asc	1a	IIIB	NED, 75	NA	+	+	+	+	pMMR/MSS	9	+13q, +20p, +20q, +Xp, +Xq	−14q, −17p, −18p, −18q
14	36/M	Colon asc	1b	IIIB	NED, 52	NA	+	+	+	+	pMMR/MSS	3	+8q, +13q	−1p, −4p, −4q
15	65/F	Colon asc	2a	IIIB	NED, 76	MSI-H	−	+	+	−	dMMR/MSI	3	+7p, +7q	−21q
16	72/M	Colon asc	2a	IIIB	DOO, 71	MSS	+	+	+	−	pMMR/MSS	13	+1q, +8q, +13q, +20p, +20q	−1p, −3p, −3q, −4p, −4q, −6p, −6q, −8p, −18q
17	61/M	Colon asc	2a	IIIB	DOO, 14	NA	+	+	+	+	pMMR/MSS	11	+6p, +7p, +13q, +20p, +20q, +Xp, +Xq	−1p, −4p, −4q, −6q, −8p, −14q, −17p, −18q, −22q
18	70/M	Colon hep flex	2b	IIIC	DOTD (DP), 23 (15)	NA	+	+	+	+	pMMR/MSS	0	+8q	0

(Continues)

TABLE 1 (Continued)

No.	Age (years)/ sex	Site	pN	Clinical stage	Follow-up, OS (months)	MS analysis	MMR immunohistochemistry				MMR/MS status	Aneuploidy score	Gains	Losses
							MLH1	MSH2	MSH6	PMS2				
19	42/M	Colon asc	0	IVA	NED (SMD), 93 (0)	MSI-H	+	+	+	−	dMMR/MSI	0	0	0
20	58/F	Caecum	0	IVA	NED (SMD), 51 (0)	NA	+	+	+	+	pMMR/MSS	2	+7p, **++12p**	−8p
21	80/M	Colon asc	1b	IVA	DOO (SMD), 20 (0)	NA	+	+	+	+	pMMR/MSS	5	+13q, +16p, +20q	−18p, −18q
22	78/F	Colon asc	2a	IVA	DOTD (SMD), 44 (0)	NA	+	+	+	+	pMMR/MSS	0	0	−8p
23	38/M	Caecum	2a	IVA	DOTD (SMD), 2 (0)	NA	+	+	+	+	pMMR/MSS	4	+13q, +20q	−4q, −18q
24	67/M	Caecum	2b	IVA	DOTD (SMD), 14 (0)	MSI-H	−	+	+	−	dMMR/MSI	4	+8p, +8q, +12p, +12q	0
25	78/F	Caecum	2b	IVA	DOTD (SMD), 7 (0)	NA	+	+	+	+	pMMR/MSS	3	+9q, +17p, +17q	−1p, −3p, −4q, −6q, −18q
26	79/M	Colon hep flex	2b	IVA	DOTD (SMD), 3 (0)	NA	+	+	+	+	pMMR/MSS	17	+2q, +7p, +7q, +11p, +12p, +13q, +18p, +18q, +20q, +Xp, +Xq, **++8q**	−1p, −2q, −3p, −4q, −5p, −5q, −8p, −9p, −17p, −17q, −21q, −22q
27	74/F[a]	Rectum	0	IIA	NED, 60	NA	+	+	−	+	dMMR/MSI	0	0	0
28	65/M	Rectum	0	IIA	NED, 45	NA	+	+	+	+	pMMR/MSS	1	+20q	0
29	72/F[a]	Rectum	0	IIA	NED, 103	NA	+	+	+	+	pMMR/MSS	1	0	−17p, −18q
30	53/M	Rectum	0	IIA	NED, 34	NA	+	+	+	+	pMMR/MSS	3	+16p, +20q	−18q
31	74/F[a]	Rectum	0	IIA	NED, 58 (36)	NA	+	+	+	+	pMMR/MSS	3	+20q	−14q, −18q
32	62/M	Rectum	0	IIA	NED, 60	NA	+	+	+	+	pMMR/MSS	1	+8q, +20q	−13q
33	72/M	Rectum	0	IIA	NED, 43	NA	+	+	+	+	pMMR/MSS	3	+5p, +8q, **++20q**	−5q, −8p
34	66/M[a]	Rectum	0	IIA	NED, 88	NA	+	+	+	+	pMMR/MSS	3	+20q	−1p, −10q, −18p, −18q
35	75/F	Rectum	0	IIA	NED, 51	NA	+	+	+	+	pMMR/MSS	3	+8q, +12q, **++13q, ++20q**	−18q
36	62/M[a]	Rectum	0	IIA	DOTD (DP), 22 (12)	NA	+	+	+	+	pMMR/MSS	4	+8p, +8q, +12p, +12q, **++7p**	0

TABLE 1 (Continued)

No.	Age (years)/ sex	Site	pN	Clinical stage	Follow-up, OS (months)	MS analysis	MMR immunohistochemistry				MMR/MS status	Aneuploidy score	Gains	Losses
							MLH1	MSH2	MSH6	PMS2				
37	78/F	Rectum	0	IIA	NED, 46	NA	+	+	+	+	pMMR/MSS	6	+8q, +13q, +20q	−3p, −8p, −9p, −18q
38	82/F	Rectum	0	IIA	DOO, 40	NA	+	+	+	+	pMMR/MSS	1	+3q, +5q, +8q, +20q	−5q, −6q, −18q
39	89/M	Rectum	0	IIA	NED, 18	NA	+	+	+	+	pMMR/MSS	6	+20p, +20q, +22q, +Xp, +Xq	−14q, −18p, −18q
40	57/F	Rectum	0	IIA	NED, 43	NA	+	+	+	+	pMMR/MSS	6	+13q	−3p, −4p, −4q, −11p, −11q, −15q, −18q
41	62/M	Rectum	0	IIA	NED, 46	NA	+	+	+	+	pMMR/MSS	7	+12p, +12q, +Xp, +Xq	−10q, −18p, −18q, −21q
42	80/M	Rectum	0	IIA	NED, 18	NA	+	+	+	+	pMMR/MSS	7	+8q, +13q, +20q, +Xp, +Xq	−5q, −8p, −18p, −18q
43	50/F	Rectum	0	IIA	Alive (DP), 47 (18)	NA	+	+	+	+	pMMR/MSS	5	+8q, +17q, +20q, +21q, +Xp, +Xq	−12q, −18p, −18q
44	70/M	Rectum	0	IIA	NED, 39	NA	+	+	+	+	pMMR/MSS	11	+13q, +17q, +20p, +20q, +Xp, +Xq	−14q, −15q, −17p, −18p, −18q
45	65/F[a]	Rectum	0	IIA	NED, 55	NA	+	+	+	+	pMMR/MSS	11	+13q, +17q, +20p, +20q	−4p, −4q, −5p, −5q, −18q, −Xp, −Xq
46	61/F[a]	Rectum	0	IIA	NED, 61	NA	+	+	+	+	pMMR/MSS	10	+1q, +7p, +7q, +13q, +20p, +20q	−1p, −1q, −4p, −4q, −18p, −18q
47	74/M	Rectum	0	IIA	NED, 53	NA	+	+	+	+	pMMR/MSS	10	+1q, +2p, +2q, +8q	−6q, −8p, −11p, −11q, −17p, −18p, −18q, −20p, −22q
48	82/F	Rectum	0	IIA	NED, 24	NA	+	+	+	+	pMMR/MSS	14	+5p, +6p, +9p, +12p, +13q, +20p, +20q	−5q, −8p, −14q, −15q, −17q, −18p, −18q
49	62/F	Rectum	0	IIA	NED, 8	NA	+	+	+	+	pMMR/MSS	16	+1q, +3p, +6p, +7p, +11p, +12p, +12q, +13q, +20p, +20q, +Xp, +Xq	−1p, −4p, −4q, −8p, −10p, −10q, −11q, −12q, −14q, −18p, −18q, −21q
50	70/M	Rectum	1a	IIIB	NED, 45	NA	+	+	+	+	pMMR/MSS	2	+7q, +8q, +9p, +11q, +12p	0
51	81/M	Rectum	1a	IIIB	NED, 25	NA	+	+	+	+	pMMR/MSS	7	+7p, +7q, +8q, +13q, **++20q**	−4p, −4q, −8p

(Continues)

TABLE 1 (Continued)

No.	Age (years)/ sex	Site	pN	Clinical stage	Follow-up, OS (months)	MS analysis	MMR immunohistochemistry				MMR/MS status	Aneuploidy score	Gains	Losses
							MLH1	MSH2	MSH6	PMS2				
52	80/F	Rectum	1a	IIIB	Alive, 20 (NA)	NA	+	+	+	+	pMMR/MSS	7	+1q, +3q, +6p, +7p, +7q, +13q, +20p	−6p, −15q, −18q, −Xp
53	77/F	Rectum	1a	IIIB	DOTD (DP), 37 (37)	NA	+	+	+	+	pMMR/MSS	11	+13q, +20p, +20q	−1p, −4p, −4q, −14q, −17p, −18p, −18q, −21q, −22q
54	63/F	Rectum	1b	IIIB	NED, 37	NA	+	+	+	+	pMMR/MSS	1	+6p, +15q, +20q, **++19q**	0
55	69/M	Rectum	1b	IIIB	NED, 42	NA	+	+	+	+	pMMR/MSS	6	+20q	−3p, −4q, −5q, −8p, −18q, −20p
56	79/M	Rectum	1b	IIIB	DOTD (DP), 39 (32)	NA	+	+	+	+	pMMR/MSS	9	+1q, +5q, +6p, +7p, +13q, +20p, +20q	−5p, −5q, −8p, −14q, −18p, −18q
57	58/F	Rectum	1b	IIIB	Alive (DP), 42 (29)	NA	+	+	+	+	pMMR/MSS	11	+9p, +9q, +13q, +16q, +20p	−5q, −8p, −14q, −15q, −17p, −17q, −18p, −18q, −22q
58	75/M[a]	Rectum	1b	IIIB	NED, 47	NA	+	+	+	+	pMMR/MSS	12	+8q, +10p, +13q, +16p, +16q, +20p	−2q, −4q, −8p, −10q, −14q, −17p, −18q, −19p, −19q, −22q
59	64/F	Rectum	1b	IIIB	Alive (DP), 43 (17)	NA	+	+	+	+	pMMR/MSS	12	+9q, +12p, +17q, +20p, +20q, +21q, +Xp	−1p, −4p, −4q, −8p, −10p, −10q, −14q, −18p, −18q
60	80/F	Rectum	2a	IIIC	NED, 26	NA	+	+	+	+	pMMR/MSS	0	0	0
61	46/M	Rectum	2b	IIIC	DOO, 20 (NA)	NA	−	+	+	−	dMMR/MSI	0	0	0
62	75/M[a]	Rectum	2b	IIIC	DOTD (DP), 8 (4)	NA	+	+	+	+	pMMR/MSS	1	+13q, +20q	0
63	67/M	Rectum	2b	IIIC	NED, 14	NA	+	+	+	+	pMMR/MSS	2	+20q	−8p, −18q
64	53/F[a]	Rectum	2b	IIIc	DOTD, 13 (NA)	MSS	+	+	+	+	pMMR/MSS	3	+12p, +12q, +20q	0

TABLE 1 (Continued)

No.	Age (years)/ sex	Site	pN	Clinical stage	Follow-up, OS (months)	MS analysis	MMR immunohistochemistry				MMR/MS status	Aneuploidy score	Gains	Losses
							MLH1	MSH2	MSH6	PMS2				
65	85/F	Rectum	2b	IIIC	DOO, 13 (11)	NA	+	+	+	+	pMMR/MSS	9	+8q, +13q, +20q	−3p, −4p, −8p, −14q, −15q, −18p, −18q
66	61/M	Rectum	2b	IIIC	Alive (DP), 34 (6)	NA	+	+	+	+	pMMR/MSS	9	+13q, +20p, +Xp, +Xq, **++8q, ++20q**	−1p, −4p, −4q, −14q, −17p, −18q
67	82/F	Rectum	2b	IIIC	DOO, 18 (NA)	NA	+	+	+	+	pMMR/MSS	7	+12q, +13q, +17q, +18p, **++8q**	−4q, −11p, −11q, −17p, −18q, −Xp, −Xq
68	82/F	Rectum	2b	IIIC	DOO (DP), 18 (15)	NA	+	+	+	+	pMMR/MSS	10	+7p, +7q, +8p, +8q, +13q, +Xq, **++20q**	−4q, −5q, −15q, −17p, −18p, −18q, −20p
69	44/M[a]	Rectum	2b	IIIC	DOTD (DP), 55 (11)	NA	+	+	+	+	pMMR/MSS	16	+7p, +7q, +13q, +17q, +20q	−1p, −1q, −3p, −3q, −4p, −4q, −9p, −9q, −14q, −15q, −18q, −20p
70	67/M	Rectum	2b	IIIC	Alive (DP), 17 (7)	NA	+	+	+	+	pMMR/MSS	17	+8q, +9p, +13q, +20p, +20q	−1p, −3p, −3q, −4p, −4q, −5q, −8p, −10q, −12q, −14q, −15q, −16q, −18q
71	74/M	Rectum	2b	IIIC	NED, 49	NA	+	+	+	+	pMMR/MSS	10	+5p, +6p, +6q, +7p, +8q, +9p, +15q, +20q, +22q, **++13q**	−2q, −4p, −4q, −5q, −8p, −15q, −18q
72	61/M	Rectum	1a	IVA	DOTD (SMD), 14 (0)	NA	+	+	+	+	pMMR/MSS	4	+20q, +Xp, +Xq	−18q
73	53/M[a]	Rectum	1a	IVA	Alive (SMD), 67 (0)	NA	+	+	+	+	pMMR/MSS	5	+5p, +8p, +8q, +20q	−1p, −5q, −8p, −15q, −18p, −18q
74	52/M	Rectum	2b	IVA	DOTD (SMD), 18 (0)	NA	+	+	+	+	pMMR/MSS	1	+20q	0

(Continues)

TABLE 1 (Continued)

No.	Age (years)/ sex	Site	pN	Clinical stage	Follow-up, OS (months)	MS analysis	MMR immunohistochemistry				MMR/MS status	Aneuploidy score	Gains	Losses
							MLH1	MSH2	MSH6	PMS2				
75	75/F	Rectum	2b	IVB	DOTD (SMD), 12 (0)	NA	+	+	+	+	pMMR/MSS	19	+2p, +2q, +3q, +5p, +8q, +12p, +13q, +20p, +20q, +Xp, +Xq	−1p, −1q, −2p, −2q, −3p, −3q, −4p, −4q, −8p, −12q, −14q, −15q, −16p, −18q, −21q, −22q

Note: High-level amplifications are in bold.

Abbreviations: asc, ascending; dMMR, deficient mismatch repair; DOO, died of other causes; DOTD, died of tumour disease; DP, disease progression; F, female; hep flex, hepatic flexure; M, male; MSI-H, microsatellite-unstable, high degree; MSS, microsatellite-stable; NA, not available; NED, no evidence of disease; OS, overall survival; pMMR, proficient mismatch repair; SMD, synchronous metastatic disease; transv, transverse.

[a]Patients included in the CAO/ARO/AIO-94 phase III trial of the German Rectal Cancer Study Group [44].

FIGURE 1 Overall survival of colorectal cancer patients stratified according to the node status and UICC stage using Kaplan–Meier analysis

imbalances, the mean aneuploidy score was significantly lower in proximal CRCs than in distal CRCs (aneuploidy score of 3.8 vs. 6.6; $p = 0.02$; Wilcoxon test; Table 2). However, when the MMR/MS status was taken into account in addition to the tumour site, no significant differences were obtained ($p > 0.05$ for the pMMR/MSS and dMMR/MSI-H tumours; Wilcoxon test; Table 2), in line with the results obtained for the total number of chromosomal imbalances.

Subsequently, we sought to identify particular chromosomal changes that might distinguish tumours by anatomical site. However, there was no universal chromosomal marker that distinguished between proximal and distal CRCs. If any, there were differences in the frequencies of chromosomal imbalances. In accordance with the lower

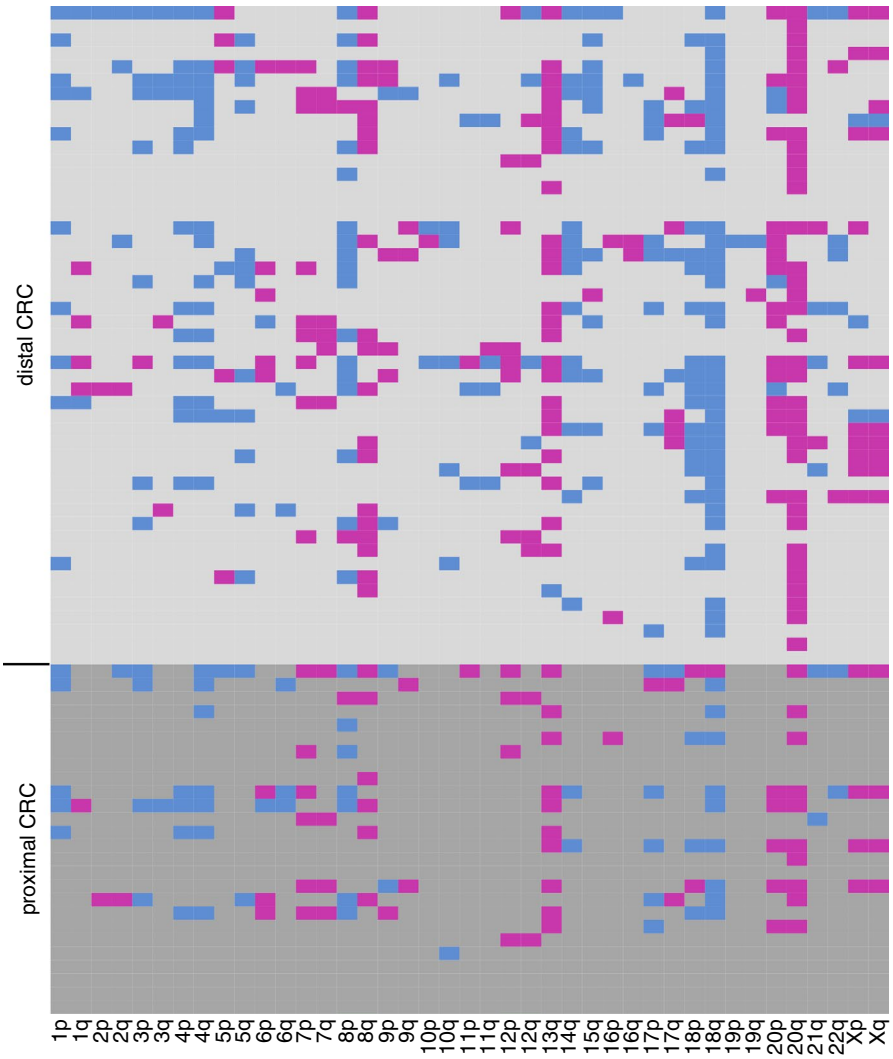

FIGURE 2 Pattern of copy number aberrations observed in 26 proximal colorectal cancers (CRCs; background in grey, bottom) and 49 distal CRCs (background in light grey, top). Losses and gains are shown in blue and purple, respectively

TABLE 2 Site-dependent differences in copy number aberrations between 26 proximal pT3 colorectal cancers (CRCs) and 49 distal pT3 CRCs

	Proximal CRC ($n = 26$)	Distal CRC ($n = 49$)	Site-dependent differences
	Mean (range)	Mean (range)	*p*-value
No. of imbalances (all)	5.3 (0–24)	8.8 (0–27)	**0.02**
No. of imbalances (pMMR/MSS)	6.8 (0–24)	9.1 (0–27)	ns
No. of imbalances (dMMR/MSI-H)	1.0 (0–4)	0.0 (0)	ns
Aneuploidy score (all)	3.8 (0–17)	6.6 (0–19)	**0.02**
Aneuploidy score (pMMR/MSS)	4.9 (0–17)	6.9 (0–19)	ns
Aneuploidy score (dMMR/MSI-H)	1.0 (0–4)	0.0 (0)	ns

Note: The total number of chromosomal imbalances (i.e. focal and arm-level copy number aberrations) and the aneuploidy score (i.e. number of apparent arm-level imbalances) are listed. Significant *p*-values are shown in bold.

Abbreviation: dMMR, deficient mismatch repair; MSI-H, microsatellite-unstable, high degree; MSS, microsatellite-stable; ns, not significant; pMMR, proficient mismatch repair.

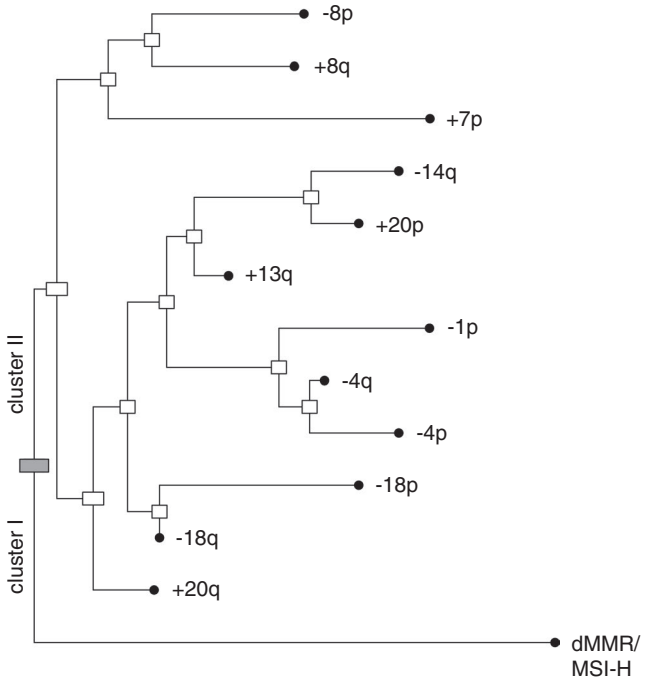

FIGURE 3 Oncogenetic tree model for the genetic evolution of proximal and distal colorectal cancers reconstructed using maximum-likelihood estimation. Events predicted to occur early are placed in proximity to the root (grey box). Cluster I marked by dMMR/MSI-H (deficient mismatch repair/high degree of microsatellite instability) and cluster II marked by chromosomal instability (CIN) are labelled

degree of chromosomal imbalances in proximal CRCs, statistical analysis revealed −18q (35% vs. 73%.; $p = 0.007$; Fisher's exact test), +20q (38% vs. 73%; $p = 0.02$; Fisher's exact test) and −15q (0% vs. 24%; $p = 0.02$; Fisher's exact test) to be less common in proximal CRCs than in distal CRCs. The overall pattern of chromosomal imbalances, however, did not differ substantially between proximal and distal CRCs (Figure 2).

Compared with pMMR/MSS CRCs, dMMR/MSI-H tumours appeared to have significantly lower levels of chromosomal imbalances (mean 8.5 for pMMR/MSS tumours vs. 0.8 for dMMR/MSI-H CRCs; $p = 0.0003$; Wilcoxon test), an association which held true for both proximal and distal CRCs. There were seven dMMR/MSI-H tumours (five proximal and two distal CRCs) with concurrent karyotype lacking apparent chromosomal imbalances, representing 71% (5/7) of proximal dMMR/MSI-H tumours and all (2/2) of the distal dMMR/MSI-H tumours. Specifically, dMMR/MSI-H CRCs presented with lower frequencies of −18q ($p = 0.0006$; Fisher's exact test), +20q ($p = 0.0006$), +13q ($p = 0.01$) and −8p ($p = 0.047$) than pMMR/MSS tumours. In comparison, only two pMMR/MSS tumours (one proximal and one distal CRC) had a karyotype without apparent copy number aberrations.

Oncogenetic tree modelling

Finally, we modelled the genetic evolution of the CRCs in our series. To this end, we took advantage of oncogenetic tree modelling. Maximum likelihood estimation was first performed for the entire cohort and considered the MMR/MS status and the 12 most common copy number aberrations observed in our cohort. The oncogenetic tree model suggested the presence of two main clusters (Figure 3). Cluster I comprised CRCs with dMMR/MSI-H, while cluster II was characterized by the presence of CIN. In the latter, four subclusters were obtained: a +8q subcluster with correlation of +7p, −8p and +8q; a +13q cluster comprising −1p, −4p, −4q, +13q, −14q and +20p; an −18q subcluster with −18p and −18q; and a +20q subcluster (Figure 3).

To model the evolution of the CRCs dependent on the tumour site, maximum-weight branching oncogenetic tree models were reconstructed separately for the proximal and distal CRCs in order to predict cancer evolution (Figure 4). The derived models support multiple possible orders of accumulation of chromosomal imbalances. As for the maximum likelihood-based model (Figure 3), the maximum-weight branching oncogenetic tree models predicted an dMMR/MSI-H cluster for both the proximal and distal CRCs (Figure 4). Moreover, for the proximal CRCs, +13q and +20q were placed close to the root, suggesting these copy number aberrations to represent early events in tumour evolution (Figure 4A). The +13q subcluster was suggested to progress via different paths. For the distal CRCs, paths via +8q, −18q and +20q were predicted, and tumours in the −18q subcluster appeared to acquire multiple further chromosomal aberrations (Figure 4B). Remarkably, gain of 8q was indicated as a rather late event in proximal CRCs, while it was modelled as an early event in distal CRCs.

Furthermore, when divided according to the number of chromosomal imbalances (≤ 10 vs. >10 aberrations), overall similar trees were built for the two groups, indicating that cases with low to moderate CIN and high CIN exhibit similar changes (Figure 5). In particular, +13q, −18q and +20q were predicted as preferentially early events, while aberration −1p, amongst others, was predicted as a late event in CRC evolution. A differential positioning, however, was observed for −17p, which was predicted to represent a late event in the low to moderate CIN group but an early event in the group showing high CIN (Figure 5).

Finally, we modelled the cytogenetic evolution dependent on the node status and distant metastatic disease using maximum-weight branching oncogenetic tree models. Again, these models shared +13q, −18q and +20q as preferentially early events irrespective of the node status (Figure 6) or presence of distant metastasis (Figure 7), respectively. However, −8p was modelled as an early event in node-positive CRCs (Figure 6B,C) but as a late event in CRCs with pN0 status (Figure 6A). Moreover, +7p and +8q occurred early in the cytogenetic evolution of CRCs presenting with synchronous and metachronous distant metastasis (Figure 7B,C). In contrast, these chromosomal imbalances were late events in CRCs that showed no clinical sign of distant metastasis (Figure 7A). Cytogenetic tree modelling thus identified distinct patterns of chromosomal imbalances dependent on tumour characteristics.

DISCUSSION

Clinico-pathological differences of right-sided and left-sided CRCs suggest different aetiological backgrounds and the existence of

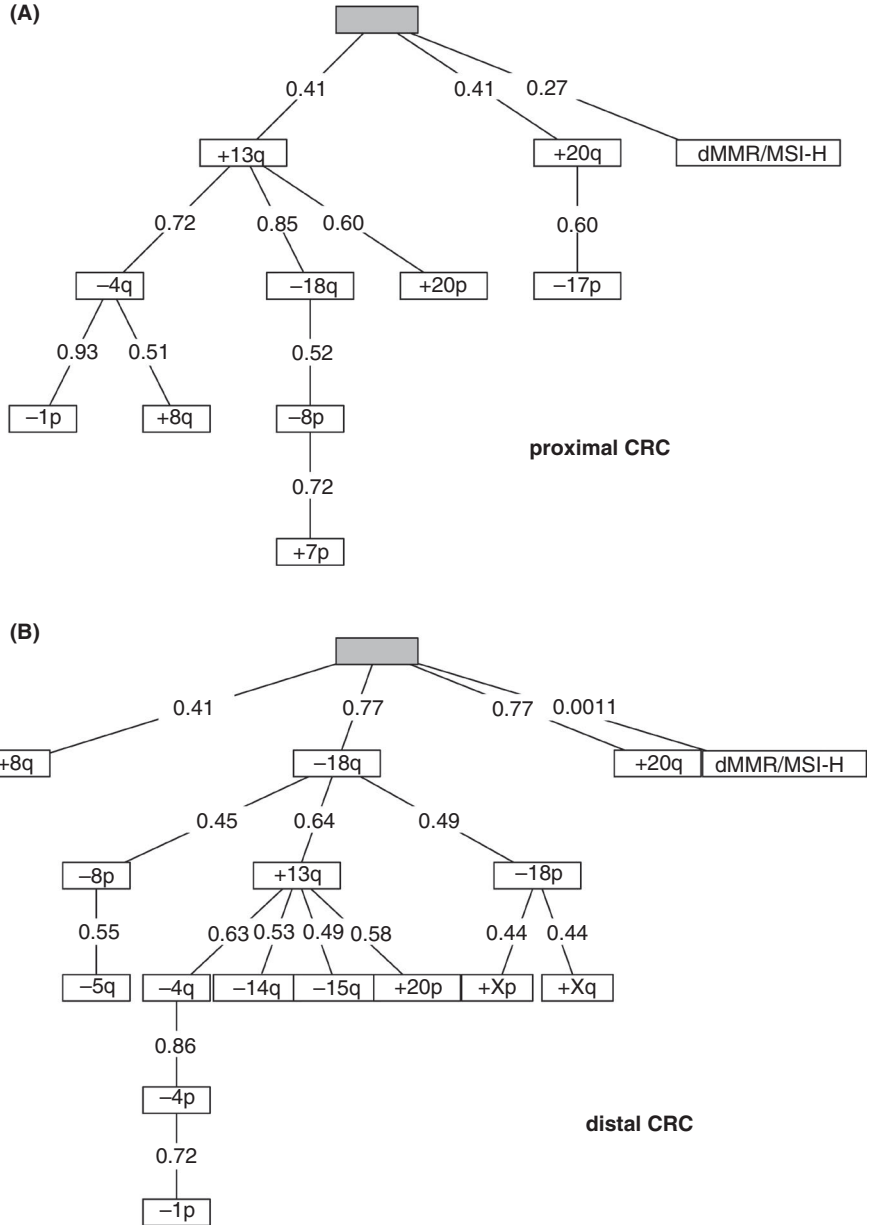

FIGURE 4 Maximum-weight branching oncogenetic tree models for proximal (A) and distal colorectal cancer (CRC) (B). Early events are located close to the root (grey boxes) of the tree. dMMR/MSI-H, deficient mismatch repair/high degree of microsatellite instability

multiple categories of CRCs [3–5,7,8,]. Herein, oncogenetic tree modelling of the MS status combined with copy number aberrations indicated that it is the type of genomic instability, i.e. CIN [10,11] or dMMR/MSI-H [19,20] that represents a central criterion in the stratification of CRCs, independent of the tumour site. Accordingly, the oncogenetic tree models presented herein predicted two similar main clusters for both proximal and distal CRCs, one cluster characterized by dMMR/MSI-H and the other cluster by multiple chromosomal imbalances.

In the present series, MMR immunohistochemistry and MSI analysis identified nine dMMR/MSI-H tumours, representing 27% of the proximal CRCs but only 4% of the distal CRCs. These dMMR/MSI-H tumours were found to have either no or a limited number of chromosomal imbalances, which supports previous observations that dMMR/MSI-H tumours present with lower degrees of chromosomal imbalances than pMMR/MSS tumours [21–24]. The significantly lower number of chromosomal imbalances and a trend toward higher rates of karyotypes without apparent copy number aberrations observed in the proximal CRC group could be attributed to the higher frequency of dMMR/MSI-H tumours at this site. Accordingly, we did not observe significant differences in the number of chromosomal imbalances when only pMMR/MSS tumours were compared.

Chromosomal imbalances identified in dMMR/MSI-H tumours in our series were gains of chromosomes 7, 8 and 12, which apparently involved whole chromosomes, in addition to a loss of 21q (note that 21p cannot be addressed with the method used). Gains of chromosomes 7 [23,24] and 12 [24] were previously observed in dMMR/MSI-H CRCs, and also whole-chromosomal gains of chromosome 8 were consistently reported for dMMR/MSI-H CRCs [23]. In contrast, it is isochromosome 8q (resulting in −8p and +8q) [51] that appears to be enriched in pMMR/MSS CRCs [52]. We did not observe gains of chromosome 13q, one of the predominant chromosomal aberrations

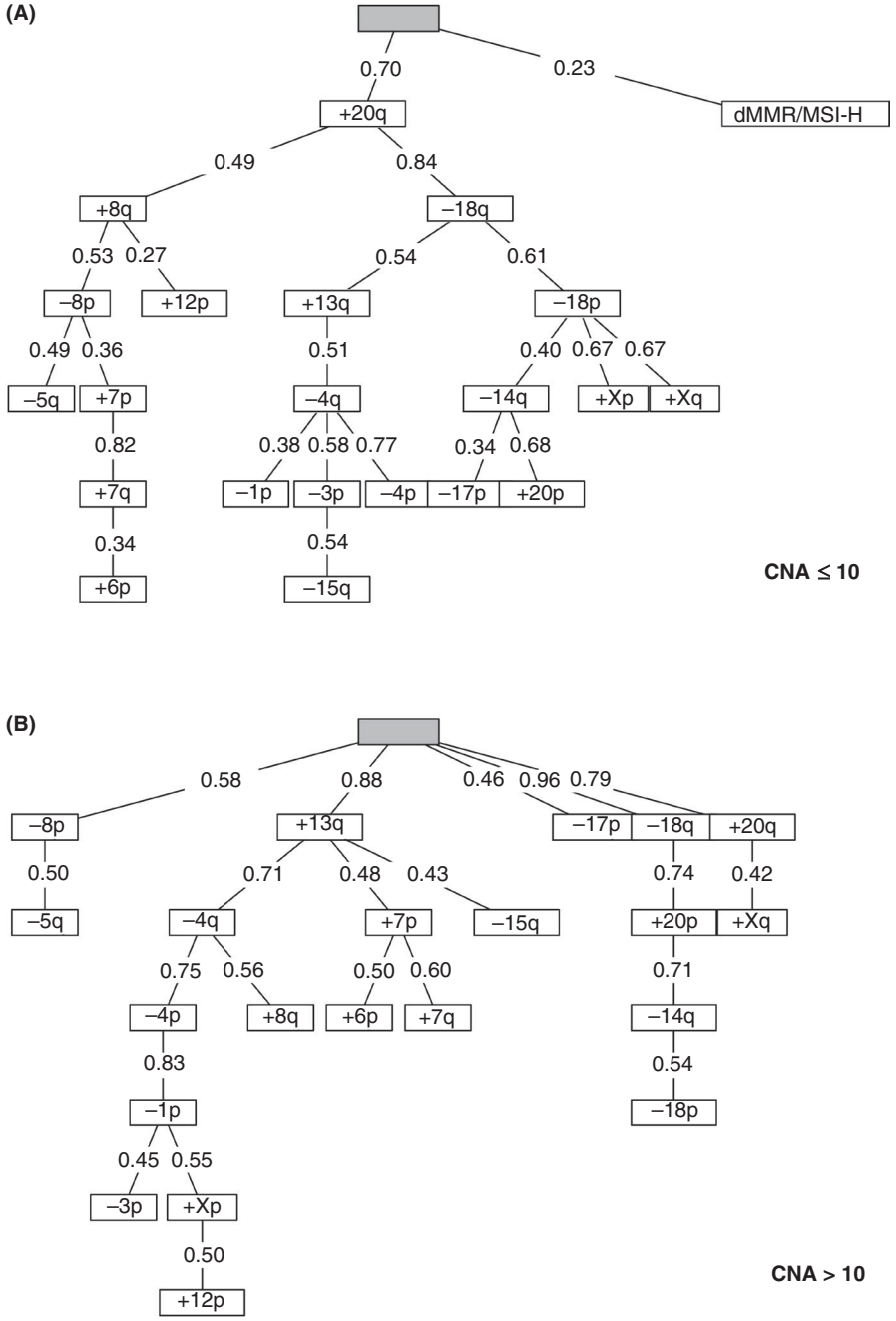

FIGURE 5 Maximum-weight branching oncogenetic tree models for colorectal cancer (CRC) with a low to moderate (A) and high degree (B) of chromosomal instability. Events close to the root (grey boxes) of the tree represent early events. A total of 10 copy number aberrations (CNA) was used as the cutoff. dMMR/MSI-H, deficient mismatch repair/high degree of microsatellite instability

found in pMMR/MSS CRCs [14], in the dMMR/MSI-H CRCs in our series. The frequency of dMMR/MSI-H CRC presenting with gains of 13q appears to differ markedly in previous reports amounting to 5%–60% [22–25]. Further studies with larger cohorts are required to address the occurrence of +13q in dMMR/MSI-H tumours. The low frequency of −18q appears to represent a consistent feature of dMMR/MSI-H CRC [22–25], in line with our results.

In the CIN subset of tumours, there was little qualitative variation in the pattern of chromosomal imbalances between proximal and distal CRCs. Our data suggested that tumours assigned to the CIN cluster can evolve through multiple, interconnected pathways: a +8q subcluster, a +13q subcluster, a +20q subcluster and a −18q subcluster. The subclusters, however, do not represent mutually exclusive pathways but rather are correlated and emerge from the root of the maximum likelihood-based oncogenetic tree as a common trunk.

Gains at 13q and 20q as well as losses at 18q observed in the CIN cluster are among the most common chromosomal imbalances identified in CRCs [14,53–60], and −18q and +20q – in addition to −8p and +8q – have been suggested to represent early events in previous tree analyses of CRCs [61]. In another study, +8q and −18 with losses at 17p were modelled to represent preferentially early events, and gains at 2q, 7p, 13q and 20q as well as losses at 4q, 8p and 14q to occur later during the evolution of the CRC [39]. While the general concept described in the latter study agrees with our series, our oncogenetic tree models favour a model in which gains at

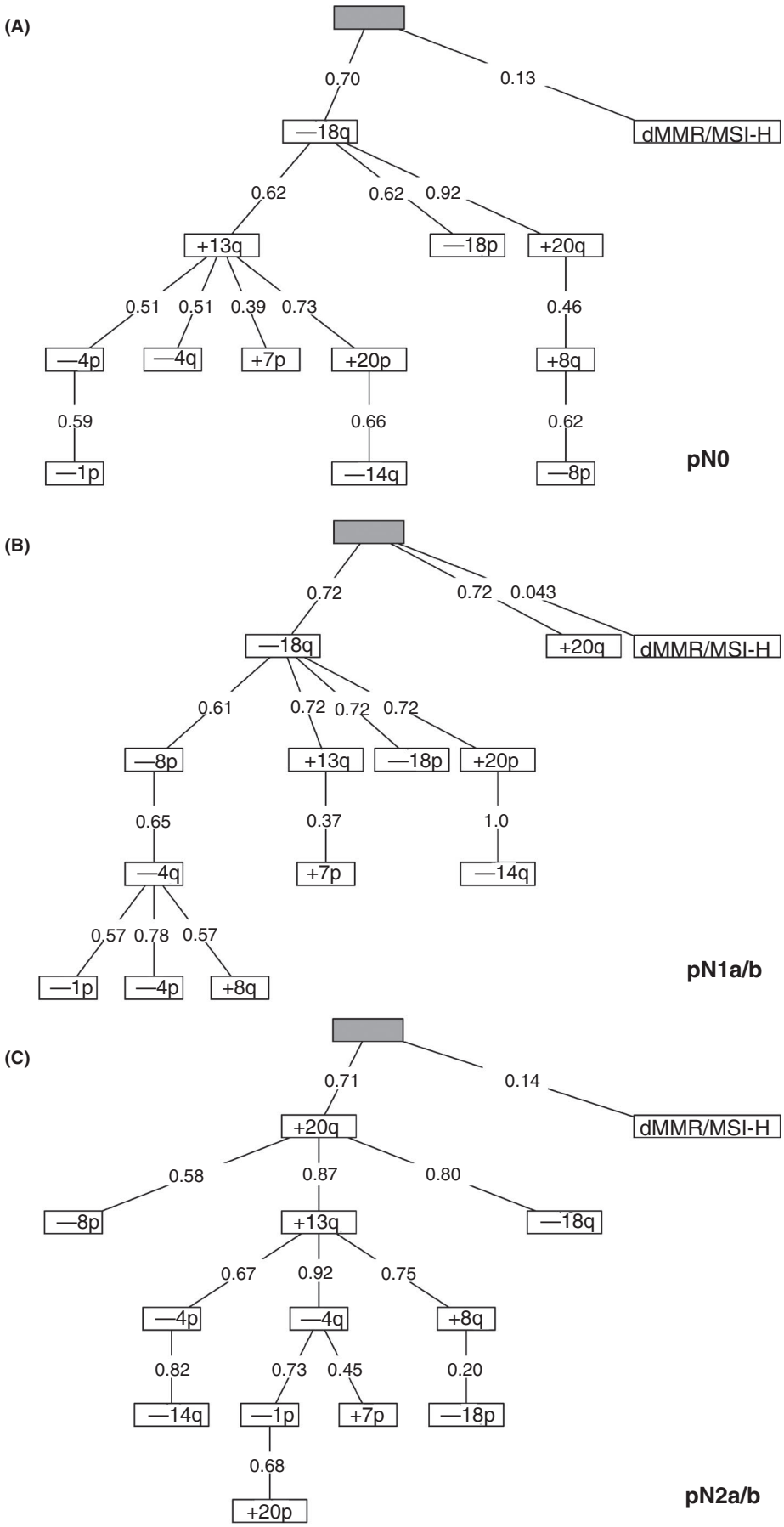

FIGURE 6 Maximum-weight branching oncogenetic tree models for colorectal cancers with negative node status (pN0) (A), pN1a/b (B) and pN2a/b (C). The root (grey boxes) of the tree is indicated. dMMR/MSI-H, deficient mismatch repair/high degree of microsatellite instability

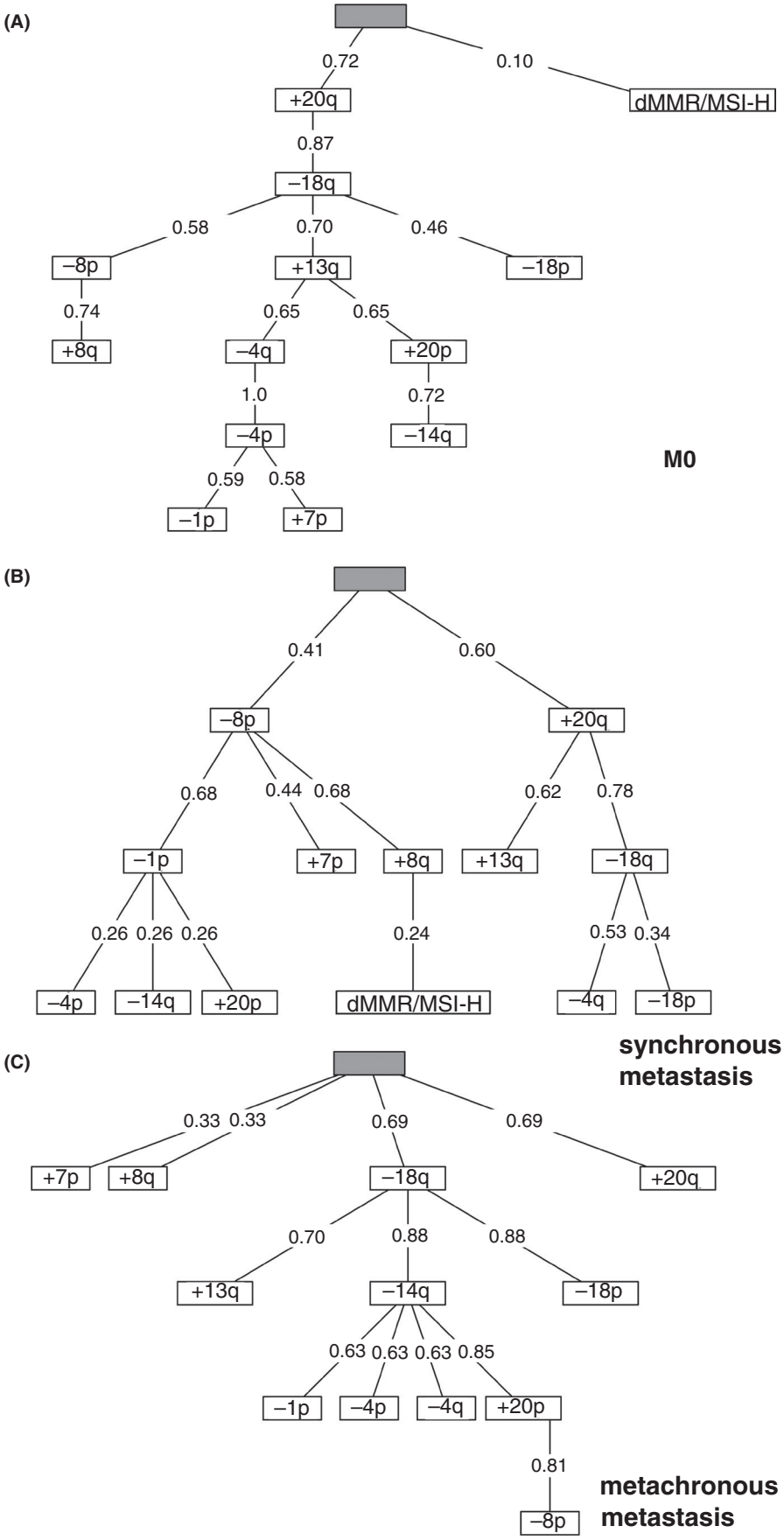

FIGURE 7 Maximum-weight branching oncogenetic tree models for colorectal cancer without distant metastasis (A), with synchronous metastasis (B) and with metachronous metastasis (C), respectively. The grey box marks the root of the tree. dMMR/MSI-H, deficient mismatch repair/high degree of microsatellite instability

20q and 13q represent early events in the development of CRC. In contrast to the aforementioned pattern of copy number aberrations in CRC, the rate of losses at 17p, which amongst others harbours the central tumour suppressor gene *TP53*, appears to vary considerably in the published cohorts [14,54,56–58,62,63]. The −17p rate in our cohort is in a similar range in a subset of these studies [56,57,63].

When the CRCs were stratified according to the number of chromosomal aberrations into a group with low to moderate CIN (≤10 aberrations) and a group with a high degree of CIN (>10 aberrations), a differential positioning of −17p in the oncogenetic tree was observed. In CRCs with low to moderate CIN, −17p was predicted as a late event, while it was predicted as an early event in CRCs with high CIN. Collectively, these results suggest a differential role of −17p in the evolution of CRCs with low to moderate CIN and high CIN, and add to a model in which multiple pathways are active in these groups. Along these lines, −17p has been previously linked to increased CIN [64].

The oncogenetic tree reconstruction following a subdivision according to the node status and distant metastatic disease suggested distinct differences in the cytogenetic evolution of CRCs. In particular, loss of the short arm of chromosome 8 was predicted as an early event in tumours with positive node status. However, we did not observe major differences in the positioning of +8q in oncogenetic trees, an aberration previously suggested to be enriched in CRC with lymph node metastasis [16]. Thus, the point in time when +8q is acquired might be less relevant for the potential of the tumour cells to form lymph node metastasis. In CRCs with synchronous and metachronous metastatic disease, gains of chromosome 8q and, in particular, of 7p, which was previously linked to liver metastasis [65], were indicated as early events in cytogenetic evolution. Of note, recent studies using paired primary CRCs and their distant metastasis are in line with a model in which tumour spreading to distant sites takes place early in the disease in at least a subset of patients [66,67].

Furthermore, our oncogenetic tree modelling attributed −1p, −4 and −5q, amongst others, as late events in tumour evolution. Hepatic metastasis was previously shown to be enriched in losses at 1p [17], and loss of chromosome 4 has been linked to advanced stages and metastatic events in patients with CRCs [65]. Loss of 5q was shown to represent an aberration acquired in brain and pulmonary metastasis of CRCs, while −5q was only rarely observed in the corresponding primary tumours [12,13], which independently provides evidence for −5q as a late event. Thus, our oncogenetic tree models captured differential evolutionary events in CRCs.

Remarkably, some of the copy number aberrations observed in the CRC series reported herein have also been demonstrated in subsets of colorectal adenomas [53,62,68–70], indicating that these chromosomal imbalances are acquired early in disease development. In a recent study, more than three quarters of the colorectal adenomas had at least one chromosomal imbalance and these aberrations included +7, +13q, +20q (14% each) and −18 (6%) [70], all of which are also observed in CRCs [14,53–59]. The aforementioned aberrations overlap well with the subclusters in our oncogenetic tree models and independently support a model in which +13q, +20q and −18q represent early events in tumour development. Of note, somatic copy number aberrations affecting chromosomes 3, 7, 9 and X have been reported in colorectal epithelium without histological evidence of neoplasia [71]. Except for gains at chromosome 7, these aberrations do not appear to be enriched in CRCs [14,53–59], and the relevance of these observations remains to be determined.

In this study, we took advantage of an approach that, in addition to the MMR/MS status, focuses on larger chromosomal copy number variations. Along these lines, recurrent, large chromosomal aberrations, often at the level of whole chromosomal arms or entire chromosomes, have been established as a major source of copy number alterations in CRCs [14,72]: about 80%–90% of CRCs present with whole chromosome or whole chromosomal arm aneuploidy [49]. Consistently, we determined in our series that 83% of the CRCs showed an apparent copy number change in at least one chromosomal arm. Note that genetic variants below the resolution of the karyotyping approach and copy number neutral loss of heterozygosity as well as certain structural variants would have been missed, as would small-scale mutations.

The pathogenetic significance of aneuploidy is only beginning to emerge [23,49,73–76]. The chromosomal regions that predominantly appear to show whole-arm imbalances in CRCs harbour several important oncogenes and tumour suppressor genes linked to tumour development [14,52,58,77]. For example, the long arm of chromosome 8 encompasses, amongst others, the oncogene *MYC*, which was found to be overexpressed in CRC [78], and the *MYC* locus was shown to belong to the major sites gained in CRC [52,58] including amplifications in a subset of cases [14]. *MYC* codes for a transcription factor favouring cell proliferation [79]. With respect to gains and amplifications of 13q, the *KLF5* gene encoding a Krüppel-like transcription factor involved in the regulation of the cell cycle in epithelial cells of the intestine [80], has been suggested as candidate oncogene for CRC pathogenesis, amongst others [14,52], as was *HNF4A* [14,52] located on chromosome 20q that encodes a transcription factor of the nuclear receptor protein family [81]. Losses at −18q have been associated with *SMAD4* [77], a member of the transforming growth factor beta signaling pathway [82]. However, as the expression level of the vast majority of genes appears to be linked to the copy number of the respective gene [83,84], additional genes in these chromosomal regions may also contribute to cancer development.

In conclusion, the present study supports the idea of different evolutionary clusters that are dominated by either CIN or dMMR/MSI-H irrespective of the tumour site and adds evidence to the concept of different genetic pathways being active in CRCs. For CRCs marked by CIN as a predominant characteristic, our oncogenetic tree models contribute to an evolutionary model of CRCs following multiple, interconnected chromosomal aberration pathways. Thus, our data support the Vogelgram concept [37], which proposes that tumour evolution of CRC is driven by the accumulation of genetic alterations in the tumour cells but also suggest a link between the timing of individual genetic events and the biological potential of the tumour cells.

FUNDING STATEMENT

This study received funding from the University Medical Center Göttingen to LF and the guest professorship programme of the University of Augsburg to MMG.

ACKNOWLEDGEMENTS

We thank Karin Hannemann for invaluable help with acquiring follow-up data. We also thank Dr Jens Kuhlgatz (Department of Surgery, Albert-Schweitzer-Hospital, Northeim, Germany), Dr Sven Detken (Northeim, Germany) and Dr Bodo Fleischer (Department of Surgery; Evangelic Hospital, Göttingen-Weende, Germany) for their cooperation in providing clinical patient data. Open access funding enabled and organized by ProjektDEAL.

CONFLICT OF INTEREST

The authors of this study are not aware of any conflict of interest related to this study.

ETHICAL APPROVAL

This study was approved by the local ethics committee.

AUTHOR CONTRIBUTIONS

Conceptualization: MMG. Investigation: MMG, BG, MC, CE, BS. Formal analysis: MMG, BS. Resources: SC, TL, LF. Visualization: MMG. Writing - original draft: MMG. Writing - review & editing: all authors. Final approval: all authors. Funding acquisition: MMG, LF. Supervision: BG, LF, BS.

DATA AVAILABILITY STATEMENT

The data that support the findings of this study are available on request from the corresponding author. The data are not publicly available due to privacy or ethical restrictions.

ORCID

Mariola Monika Golas https://orcid.org/0000-0003-2477-9277

Bjoern Sander https://orcid.org/0000-0001-8495-2321

REFERENCES

1. Fitzmaurice C, Abate D, Abbasi N, Abbastabar H, Abd-Allah F, Abdel-Rahman O, et al. Global, regional, and national cancer incidence, mortality, years of life lost, years lived with disability, and disability-adjusted life-years for 29 cancer groups, 1990 to 2017: a systematic analysis for the global burden of disease study. JAMA Oncol. 2019;5(12):1749–68.
2. Siegel RL, Miller KD, Goding Sauer A, Fedewa SA, Butterly LF, Anderson JC, et al. Colorectal cancer statistics, 2020. CA Cancer J Clin. 2020;70(3):145–64.
3. Bufill JA. Colorectal cancer: evidence for distinct genetic categories based on proximal or distal tumor location. Ann Intern Med. 1990;113(10):779–88.
4. Yang SY, Cho MS, Kim NK. Difference between right-sided and left-sided colorectal cancers: from embryology to molecular subtype. Expert Rev Anticancer Ther. 2018;18(4):351–8.
5. Lee MS, Menter DG, Kopetz S. Right versus left colon cancer biology: integrating the consensus molecular subtypes. J Natl Compr Canc Netw. 2017;15(3):411–9.
6. Yamauchi M, Morikawa T, Kuchiba A, Imamura YU, Qian ZR, Nishihara R, et al. Assessment of colorectal cancer molecular features along bowel subsites challenges the conception of distinct dichotomy of proximal versus distal colorectum. Gut. 2012;61(6):847–54.
7. Li Y, Feng Y, Dai W, Li Q, Cai S, Peng J. Prognostic effect of tumor sidedness in colorectal cancer: a SEER-based analysis. Clin Colorectal Cancer. 2019;18(1):e104–e16.
8. Paschke S, Jafarov S, Staib L, Kreuser E-D, Maulbecker-Armstrong C, Roitman M, et al. Are colon and rectal cancer two different tumor entities? A proposal to abandon the term colorectal cancer. Int J Mol Sci. 2018;19(9):2577.
9. Guinney J, Dienstmann R, Wang X, de Reyniès A, Schlicker A, Soneson C, et al. The consensus molecular subtypes of colorectal cancer. Nat Med. 2015;21(11):1350–6.
10. Reichmann A, Martin P, Levin B. Chromosomal banding patterns in human large bowel cancer. Int J Cancer. 1981;28(4):431–40.
11. Muleris M, Salmon RJ, Zafrani B, Girodet J, Dutrillaux B. Consistent deficiencies of chromosome 18 and of the short arm of chromosome 17 in eleven cases of human large bowel cancer: a possible recessive determinism. Ann Genet. 1985;28(4):206–13.
12. Gutenberg A, Gerdes JS, Jung K, Sander B, Gunawan B, Bock HC, et al. High chromosomal instability in brain metastases of colorectal carcinoma. Cancer Genet Cytogenet. 2010;198(1):47–51.
13. Danner BC, Gerdes JS, Jung K, Sander B, Enders C, Liersch T, et al. Comparison of chromosomal aberrations in primary colorectal carcinomas to their pulmonary metastases. Cancer Genet. 2011;204(3):122–8.
14. Cancer Genome Atlas N. Comprehensive molecular characterization of human colon and rectal cancer. Nature. 2012;487(7407):330–7.
15. Ried T, Knutzen R, Steinbeck R, Blegen H, Schröck E, Heselmeyer K, et al. Comparative genomic hybridization reveals a specific pattern of chromosomal gains and losses during the genesis of colorectal tumors. Genes Chromosomes Cancer. 1996;15(4):234–45.
16. Ghadimi BM, Grade M, Liersch T, Langer C, Siemer A, Fuzesi L, et al. Gain of chromosome 8q23-24 is a predictive marker for lymph node positivity in colorectal cancer. Clin Cancer Res. 2003;9(5):1808–14.
17. Ghadimi BM, Grade M, Monkemeyer C, Kulle B, Gaedcke J, Gunawan B, et al. Distinct chromosomal profiles in metastasizing and non-metastasizing colorectal carcinomas. Cell Oncol. 2006;28(5–6):273–81.
18. Young J, Leggett B, Gustafson C, Ward M, Searle J, Thomas L, et al. Genomic instability occurs in colorectal carcinomas but not in adenomas. Hum Mutat. 1993;2(5):351–4.
19. Thibodeau SN, Bren G, Schaid D. Microsatellite instability in cancer of the proximal colon. Science. 1993;260(5109):816–9.
20. Shibata D, Peinado MA, Ionov Y, Malkhosyan S, Perucho M. Genomic instability in repeated sequences is an early somatic event in colorectal tumorigenesis that persists after transformation. Nat Genet. 1994;6(3):273–81.
21. Schlegel J, Stumm G, Scherthan H, Bocker T, Zirngibl H, Ruschoff J, et al. Comparative genomic in situ hybridization of colon carcinomas with replication error. Cancer Res. 1995;55(24):6002–5.
22. Li LS, Kim N-G, Kim SH, Park C, Kim H, Kang HJ, et al. Chromosomal imbalances in the colorectal carcinomas with microsatellite instability. Am J Pathol. 2003;163(4):1429–36.
23. Barresi V, Cinnirella G, Valenti G, Spampinato G, Musso N, Castorina S, et al. Gene expression profiles in genome instability-based classes of colorectal cancer. BMC Cancer. 2018;18(1):1265.
24. Sveen A, Johannessen B, Tengs T, Danielsen SA, Eilertsen IA, Lind GE, et al. Multilevel genomics of colorectal cancers with microsatellite instability-clinical impact of JAK1 mutations and consensus molecular subtype 1. Genome Med. 2017;9(1):46.
25. Trautmann K, Terdiman JP, French AJ, Roydasgupta R, Sein N, Kakar S, et al. Chromosomal instability in microsatellite-unstable and stable colon cancer. Clin Cancer Res. 2006;12(21):6379–85.

26. Liu BO, Nicolaides NC, Markowitz S, Willson JKV, Parsons RE, Jen J, et al. Mismatch repair gene defects in sporadic colorectal cancers with microsatellite instability. Nat Genet. 1995;9(1):48–55.
27. Ligtenberg MJL, Kuiper RP, Chan TL, Goossens M, Hebeda KM, Voorendt M, et al. Heritable somatic methylation and inactivation of MSH2 in families with Lynch syndrome due to deletion of the 3' exons of TACSTD1. Nat Genet. 2009;41(1):112–7.
28. Fishel R, Lescoe MK, Rao M, Copeland NG, Jenkins NA, Garber J, et al. The human mutator gene homolog MSH2 and its association with hereditary nonpolyposis colon cancer. Cell. 1993;75(5):1027–38.
29. Leach FS, Nicolaides NC, Papadopoulos N, Liu BO, Jen J, Parsons R, et al. Mutations of a mutS homolog in hereditary nonpolyposis colorectal cancer. Cell. 1993;75(6):1215–25.
30. Bronner CE, Baker SM, Morrison PT, Warren G, Smith LG, Lescoe MK, et al. Mutation in the DNA mismatch repair gene homologue hMLH1 is associated with hereditary non-polyposis colon cancer. Nature. 1994;368(6468):258–61.
31. Papadopoulos N, Nicolaides N, Wei Y, Ruben S, Carter K, Rosen C, et al. Mutation of a mutL homolog in hereditary colon cancer. Science. 1994;263(5153):1625–9.
32. Kane MF, Loda M, Gaida GM, Lipman J, Mishra R, Goldman H, et al. Methylation of the hMLH1 promoter correlates with lack of expression of hMLH1 in sporadic colon tumors and mismatch repair-defective human tumor cell lines. Cancer Res. 1997;57(5):808–11.
33. Herman JG, Umar A, Polyak K, Graff JR, Ahuja N, Issa J-P J, et al. Incidence and functional consequences of hMLH1 promoter hypermethylation in colorectal carcinoma. Proc Natl Acad Sci USA. 1998;95(12):6870–5.
34. Cunningham JM, Christensen ER, Tester DJ, Kim CY, Roche PC, Burgart LJ, Thibodeau SN. Hypermethylation of the hMLH1 promoter in colon cancer with microsatellite instability. Cancer Res. 1998;58(15):3455–60.
35. Toyota M, Ahuja N, Ohe-Toyota M, Herman JG, Baylin SB, Issa JP. CpG island methylator phenotype in colorectal cancer. Proc Natl Acad Sci USA. 1999;96(15):8681–6.
36. Kim JH, Rhee Y-Y, Bae J-M, Kwon H-J, Cho N-Y, Kim MJ, et al. Subsets of microsatellite-unstable colorectal cancers exhibit discordance between the CpG island methylator phenotype and MLH1 methylation status. Mod Pathol. 2013;26(7):1013–22.
37. Fearon ER, Vogelstein B. A genetic model for colorectal tumorigenesis. Cell. 1990;61(5):759–67.
38. Sweeney C, Boucher KM, Samowitz WS, Wolff RK, Albertsen H, Curtin K, et al. Oncogenetic tree model of somatic mutations and DNA methylation in colon tumors. Genes Chromosomes Cancer. 2009;48(1):1–9.
39. Gerstung M, Jolly C, Leshchiner I, Dentro SC, Gonzalez S, Rosebrock D, et al. The evolutionary history of 2,658 cancers. Nature. 2020;578(7793):122–8.
40. von Heydebreck A, Gunawan B, Fuzesi L. Maximum likelihood estimation of oncogenetic tree models. Biostatistics. 2004;5(4):545–56.
41. Szabo A, Boucher K. Estimating an oncogenetic tree when false negatives and positives are present. Math Biosci. 2002;176(2):219–36.
42. Desper R, Jiang F, Kallioniemi OP, Moch H, Papadimitriou CH, Schaffer AA. Inferring tree models for oncogenesis from comparative genome hybridization data. J Comput Biol. 1999;6(1):37–51.
43. Union for International Cancer Control. In: Brierley JD, Gospodarowicz MK, Wittekind C, editors: TNM Classification of Malignant Tumours. 8th ed. Oxford: Wiley-Blackwell; 2017.
44. Sauer R, Becker H, Hohenberger W, Rödel C, Wittekind C, Fietkau R, et al. Preoperative versus postoperative chemoradiotherapy for rectal cancer. N Engl J Med. 2004;351(17):1731–40.
45. Sauer R, Liersch T, Merkel S, Fietkau R, Hohenberger W, Hess C, et al. Preoperative versus postoperative chemoradiotherapy for locally advanced rectal cancer: results of the German CAO/ARO/AIO-94 randomized phase III trial after a median follow-up of 11 years. J Clin Oncol. 2012;30(16):1926–33.
46. Murphy KM, Zhang S, Geiger T, Hafez MJ, Bacher J, Berg KD, et al. Comparison of the microsatellite instability analysis system and the Bethesda panel for the determination of microsatellite instability in colorectal cancers. J Mol Diagn. 2006;8(3):305–11.
47. Rudlowski C, Schulten H-J, Golas MM, Sander B, Barwing R, Palandt J-E, et al. Comparative genomic hybridization analysis on male breast cancer. Int J Cancer. 2006;118(10):2455–60.
48. Kallioniemi O-P, Kallioniemi A, Piper J, Isola J, Waldman FM, Gray JW, et al. Optimizing comparative genomic hybridization for analysis of DNA sequence copy number changes in solid tumors. Genes Chromosomes Cancer. 1994;10(4):231–43.
49. Taylor AM, Shih J, Ha G, Gao GF, Zhang X, Berger AC, et al. Genomic and functional approaches to understanding cancer aneuploidy. Cancer Cell. 2018;33(4):676–89 e3.
50. Ihaka R, Gentleman R. R: a language for data analysis and graphics. J Comput Graph Stat. 1996;5(3):299–314.
51. Ferti AD, Panani AD, Raptis S. Cytogenetic study of rectosigmoidal adenocarcinomas. Cancer Genet Cytogenet. 1988;34(1):101–9.
52. Palin K, Pitkänen E, Turunen M, Sahu B, Pihlajamaa P, Kivioja T, et al. Contribution of allelic imbalance to colorectal cancer. Nat Commun. 2018;9(1):3664.
53. Meijer GA, Hermsen MA, Baak JP, van Diest PJ, Meuwissen SG, Belien JA, et al. Progression from colorectal adenoma to carcinoma is associated with non-random chromosomal gains as detected by comparative genomic hybridisation. J Clin Pathol. 1998;51(12):901–9.
54. Muleris M, Salmon R-J, Dutrillaux A-M, Vielh P, Zafrani B, Girodet J, et al. Characteristic chromosomal imbalances in 18 near-diploid colorectal tumors. Cancer Genet Cytogenet. 1987;29(2):289–301.
55. Paredes-Zaglul A, Kang JJ, Essig YP, Mao W, Irby R, Wloch M, et al. Analysis of colorectal cancer by comparative genomic hybridization: evidence for induction of the metastatic phenotype by loss of tumor suppressor genes. Clin Cancer Res. 1998;4(4):879–86.
56. De Angelis PM, Clausen OP, Schjolberg A, Stokke T. Chromosomal gains and losses in primary colorectal carcinomas detected by CGH and their associations with tumour DNA ploidy, genotypes and phenotypes. Br J Cancer. 1999;80(3–4):526–35.
57. De Angelis PM, Stokke T, Beigi M, Mjaland O, Clausen OP. Prognostic significance of recurrent chromosomal aberrations detected by comparative genomic hybridization in sporadic colorectal cancer. Int J Colorectal Dis. 2001;16(1):38–45.
58. Nakao K, Mehta KR, Fridlyand J, Moore DH, Jain AN, Lafuente A, et al. High-resolution analysis of DNA copy number alterations in colorectal cancer by array-based comparative genomic hybridization. Carcinogenesis. 2004;25(8):1345–57.
59. Joosse SA, Souche F-R, Babayan A, Gasch C, Kerkhoven RM, Ramos J, et al. Chromosomal aberrations associated with sequential steps of the metastatic cascade in colorectal cancer patients. Clin Chem. 2018;64(10):1505–12.
60. Barresi V, Castorina S, Musso N, Capizzi C, Luca T, Privitera G, et al. Chromosomal instability analysis and regional tumor heterogeneity in colon cancer. Cancer Genet. 2017;210:9–21.
61. Li X, Chen J, Lu B, Peng S, Desper R, Lai M. 8p12-23 and +20q are predictors of subtypes and metastatic pathways in colorectal cancer: construction of tree models using comparative genomic hybridization data. OMICS. 2011;15(1–2):37–47.
62. Hermsen M, Postma C, Baak J, Weiss M, Rapallo A, Sciutto A, et al. Colorectal adenoma to carcinoma progression follows multiple pathways of chromosomal instability. Gastroenterology. 2002;123(4):1109–19.
63. Rooney PH, Boonsong A, McKay JA, Marsh S, Stevenson DAJ, Murray GI, et al. Colorectal cancer genomics: evidence for multiple genotypes which influence survival. Br J Cancer. 2001;85(10):1492–8.

64. Xia LC, Van Hummelen P, Kubit M, Lee HoJoon, Bell JM, Grimes SM, et al. Whole genome analysis identifies the association of TP53 genomic deletions with lower survival in Stage III colorectal cancer. Sci Rep. 2020;10(1):5009.
65. Diep CB, Kleivi K, Ribeiro FR, Teixeira MR, Lindgjaerde OC, Lothe RA. The order of genetic events associated with colorectal cancer progression inferred from meta-analysis of copy number changes. Genes Chromosomes Cancer. 2006;45(1):31–41.
66. Alves JM, Prado-Lopez S, Cameselle-Teijeiro JM, Posada D. Rapid evolution and biogeographic spread in a colorectal cancer. Nat Commun. 2019;10(1):5139.
67. Hu Z, Ding J, Ma Z, Sun R, Seoane JA, Scott Shaffer J, et al. Quantitative evidence for early metastatic seeding in colorectal cancer. Nat Genet. 2019;51(7):1113–22.
68. Leslie A, Stewart A, Baty DU, Mechan D, McGreavey L, Smith G, et al. Chromosomal changes in colorectal adenomas: relationship to gene mutations and potential for clinical utility. Genes Chromosomes Cancer. 2006;45(2):126–35.
69. Lips EH, de Graaf EJ, Tollenaar R, van Eijk R, Oosting J, Szuhai K, et al. Single nucleotide polymorphism array analysis of chromosomal instability patterns discriminates rectal adenomas from carcinomas. J Pathol. 2007;212(3):269–77.
70. Fiedler D, Heselmeyer-Haddad K, Hirsch D, Hernandez LS, Torres I, Wangsa D, et al. Single-cell genetic analysis of clonal dynamics in colorectal adenomas indicates CDX2 gain as a predictor of recurrence. Int J Cancer. 2019;144(7):1561–73.
71. Lee-Six H, Olafsson S, Ellis P, Osborne RJ, Sanders MA, Moore L, et al. The landscape of somatic mutation in normal colorectal epithelial cells. Nature. 2019;574(7779):532–7.
72. Bond CE, Nancarrow DJ, Wockner LF, Wallace L, Montgomery GW, Leggett BA, et al. Microsatellite stable colorectal cancers stratified by the BRAF V600E mutation show distinct patterns of chromosomal instability. PLoS One. 2014;9(3):e91739.
73. Davoli T, Xu A, Mengwasser K, Sack L, Yoon J, Park P, et al. Cumulative haploinsufficiency and triplosensitivity drive aneuploidy patterns and shape the cancer genome. Cell. 2013;155(4):948–62.
74. Davoli T, Uno H, Wooten EC, Elledge SJ. Tumor aneuploidy correlates with markers of immune evasion and with reduced response to immunotherapy. Science. 2017;355(6322):eaaf8399.
75. Condorelli DF, Spampinato G, Valenti G, Musso N, Castorina S, Barresi V. Positive caricature transcriptomic effects associated with broad genomic aberrations in colorectal cancer. Sci Rep. 2018;8(1):14826.
76. Condorelli DF, Privitera AP, Barresi V. Chromosomal density of cancer up-regulated genes, aberrant enhancer activity and cancer fitness genes are associated with transcriptional *cis*-effects of broad copy number gains in colorectal cancer. Int J Mol Sci. 2019;20(18):4652.
77. Thiagalingam S, Lengauer C, Leach FS, Schutte M, Hahn SA, Overhauser J, et al. Evaluation of candidate tumour suppressor genes on chromosome 18 in colorectal cancers. Nat Genet. 1996;13(3):343–6.
78. Erisman MD, Rothberg PG, Diehl RE, Morse CC, Spandorfer JM, Astrin SM. Deregulation of c-myc gene expression in human colon carcinoma is not accompanied by amplification or rearrangement of the gene. Mol Cell Biol. 1985;5(8):1969–76.
79. Eilers M, Schirm S, Bishop JM. The MYC protein activates transcription of the alpha-prothymosin gene. EMBO J. 1991;10(1):133–41.
80. Nandan MO, Chanchevalap S, Dalton WB, Yang VW. Kruppel-like factor 5 promotes mitosis by activating the cyclin B1/Cdc2 complex during oncogenic Ras-mediated transformation. FEBS Lett. 2005;579(21):4757–62.
81. Sladek FM, Zhong WM, Lai E, Darnell JE Jr. Liver-enriched transcription factor HNF-4 is a novel member of the steroid hormone receptor superfamily. Genes Dev. 1990;4(12B):2353–65.
82. Zhou S, Buckhaults P, Zawel L, Bunz F, Riggins G, Dai JL, et al. Targeted deletion of Smad4 shows it is required for transforming growth factor beta and activin signaling in colorectal cancer cells. Proc Natl Acad Sci USA. 1998;95(5):2412–6.
83. Grade M, Hörmann P, Becker S, Hummon AB, Wangsa D, Varma S, et al. Gene expression profiling reveals a massive, aneuploidy-dependent transcriptional deregulation and distinct differences between lymph node-negative and lymph node-positive colon carcinomas. Cancer Res. 2007;67(1):41–56.
84. Fehrmann RSN, Karjalainen JM, Krajewska M, Westra H-J, Maloney D, Simeonov A, et al. Gene expression analysis identifies global gene dosage sensitivity in cancer. Nat Genet. 2015;47(2):115–25.

How to cite this article: Golas MM, Gunawan B, Cakir M, Cameron S, Enders C, Liersch T, et al. Evolutionary patterns of chromosomal instability and mismatch repair deficiency in proximal and distal colorectal cancer. Colorectal Dis. 2022;24:157–176. https://doi.org/10.1111/codi.15946